A Comparative Study of Pt Depositing Methods (Chemical Reduction vs Photo-Assisted Deposition) onto TiO$_2$ Nanoparticles for Hydrogen Photo-Production

Ratnawati[1,], Slamet[2], Viona Wongso[2], Jarnuzi Gunlazuardi[3] & Muhammad Ibadurrohman[2]

[1] Department of Chemical Engineering, Institut Teknologi Indonesia, Jalan Puspitek Setu, Serpong,Tangerang Selatan 15320, Indonesia
[2] Department of Chemical Engineering, Faculty of Engineering, Universitas Indonesia, Kampus Baru UI, Depok 16424, Indonesia
[3] Department of Chemistry, Faculty of Mathematics and Sciences, Universitas Indonesia, Kampus Baru UI, Depok 16424, Indonesia
*E-mail: ratnawati.tk@iti.ac.id

Highlights:

- The preparation method plays a major role in Pt deposition efficiency, Pt dispersion, and H$_2$ generation.
- Depositing Pt on TiO$_2$ reduces the band gap and inhibits the recombination.
- Pt-TiO$_2$-CR could increase the production of H$_2$ up to 1.65 times compared with Pt-TiO$_2$-PD.

Abstract. In this paper, we report a comparative study on two methods (chemical reduction and photo-assisted deposition) of incorporating Pt onto TiO$_2$ nanoparticles (TNP) for H$_2$ generation. The phase structure of the photocatalysts was scrutinized utilizing TEM and XRD. The degree of dispersion of Pt on the TNP was calculated by a pulse chemisorption technique using TPDRO equipment. The results provided by TEM imagery, EDX spectra, elemental mapping, and AAS confirmed the successful deposition of Pt on TNP. XRD patterns confirmed an anatase and rutile crystallite structure, while UV-Vis spectra showed reduction of the bandgap from a typical value of 3.2 eV to ca. 2.9 eV. It was found that there is a correlation between the deposited Pt and dispersed Pt on the TNP with H$_2$ generation. The chemical reduction method offered a higher degree of Pt deposition, resulting in a 2.75 times larger amount of deposited Pt compared to photodeposition. This feature is perceived to contribute a higher H$_2$ yield (3,283 µmol) at 1 w% of Pt loading.

Keywords: *chemical reduction; hydrogen; photodeposition; platinum; TNP.*

1   Introduction

Energy and the environment have become crucial issues over the past few decades, mostly due to excessive exploitation of fossil-based fuels [1,2]. In recent years, hydrogen has attracted much attention, as it is a promising candidate for the replacement of fossil-based fuels, owing to its clean nature and the rapid development of fuel cells, for which hydrogen is the main fuel [3-8]. Tremendous efforts have been made on finding the most suitable technology to generate H_2. H_2 should be produced from renewable sources, e.g., water and biomass feedstock, via a benign pathway such as photocatalysis [3,5-7]. Utilizing solar energy for photocatalysis in producing hydrogen is perceived to be an ideal strategy as a conventional hydrogen route. Introducing organic and inorganic sacrificial agents in a cost-effective photocatalytic reaction system could enhance hydrogen generation from both kinetic and thermodynamic viewpoints [2,5,6,9].

Alcohols have been utilized as sacrificial agent due to their affinity towards photocatalytic reactions. The oxidation of alcohols such as glycerol suppresses the recombination of photogenerated electrons-holes [2,5,6,10-13]. To date, glycerol has been regarded as waste, however, it can be used as a renewable resource in H_2 production [5]. Thus, the production of H_2 and waste removal are expected to occur simultaneously [5,9]. It can serve as a reactant that undergoes hole-driven oxidation reactions, thus obstructing electron-hole recombination [9,14] and suppressing the O_2-H_2 back reaction to water [15,16]. The principle of water splitting, or photo-reforming of sacrificial agents is that when a semiconductor such as TiO_2 is contacted with H_2O that contains a sacrificial agent, an electron in the conduction band can reduce the water to produce H_2 if the level of the conduction band is more negative compared to the H^+/H_2 reduction potential [9]. Liquids such as ethylene glycol, acetone, acetol, acetaldehyde, acetic acid, ethanol, and methanol, and gases such as methane, ethane, and CO are some intermediate products that evolve in the glycerol photo-reforming on Pt-TiO_2 as reported by previous studies [4,16].

TiO_2 is arguably the most promising and versatile material for photocatalysis because of its low cost, high photocatalytic activity, photostability, and non-toxicity [2,17,18]. However, it has high-rate recombination of photo-generated electron-hole pairs and can only absorb UV light (the bandgap of TiO_2 is 3.2 eV for anatase and 3.0 eV for rutile) are not ideal for solar application because only 3 to 5 % of UV light is present in solar energy [2,18-20]. Serious efforts have been conducted by loading noble metals such as Pt, Pd, Au, Rh, Ru, and Ag to hamper the rapid recombination of electron holes as well as to narrow the bandgap or activity under visible light illumination [6,10,11,21]. A noble metal with a larger work function and a lower Fermi level than TiO_2 would more easily trap electrons [21,22].

A Comparative Study of Pt Depositing Methods (Chemical Reduction Vs Photo-Assisted Deposition) Onto Tio2 Nanoparticle for Hydrogen Photo-Production

Among the noble metals, Pt has the largest work function (5.65 eV) and is a promising co-catalyst as electron trapper [6,17,22]. It also has low overpotential for solar harvesting fuel generation and is very stable [23]. Platinization of TiO_2 can be done with many methods, such as Pt ion-exchange, incipient wetness, chemical reduction, and photodeposition on TiO_2 nanotubes/TNT [21,24-26]. Wet/incipient impregnation, precipitation, photochemical deposition, impregnation, and sol-gel methods for decorating Pt on TiO_2 nanoparticles/TNP [21,26], modified photo irradiation-reduction, Pt photodeposition on TiO_2 nanotube arrays/TNTA have also been conducted. On the other hand, chemical reduction and photodeposition methods have been reported as effective and common techniques for depositing Pt on TNP [5,6,24]. The suspended photocatalytic system has benefits in terms of its inexpensiveness and easy operation. Our previous study used these two methods on TiO_2 nanotube arrays/TNTA [4] for H_2 generation.

It is urgent to study these two methods in detail and provide a comparison to find the most effective method for depositing Pt on TNP, due to its expensiveness, especially for hydrogen production from glycerol-water solution. Detailed studies comparing the two methods, evaluating the characteristics and their application to produce hydrogen with glycerol as a sacrificial agent have rarely been done. The previous studies that have been conducted on Pt-TNP/TNT as a photocatalyst for hydrogen production are presented in Table 1.

Table 1 Previous studies on Pt-TNP/TNT as a photocatalyst for hydrogen production.

Photocatalyst/Ref	Doping method	Sacrificial agent	H_2 generation (4 hours)
Pt-TNP, 1 g/L Pt-TNP, 1 g/L (this study)	Photodeposition Chemical Reduction	Glycerol	1.988 mmol 3.283 mmol
Flourinated Pt- TNP, 1.5 g/L, [5]	Photodeposition	Glycerol	8.4 mmol
Pt-TNT, 1g/L [6]	Photodeposition	Butyric acid	2 mmol
Pt-TNP, 1g/L[11]	Photodeposition	Ethylene glycol	6 mmol
Pt-TNT [24]	Chemical Reduction	Ethanol	30 mmol/ h/g cat
Pt-TNT [21]	Photodeposition/ Chemical Reduction	Glycerol	173 mmol/ h/g cat

Herein, we performed Pt deposition on the surface of TiO_2-P25 or TNP using chemical reduction with $NaBH_4$ as reduction agent (Pt-TNP-CR) and photodeposition with the electron as reductor (Pt-TNP-PD) to enhance the

photocatalytic performance in producing hydrogen from 10 v% glycerol solution as a model of biodiesel waste. Based on the above-mentioned data and the information in the previous paragraphs, we claim that the comparison of deposition methods is the academic novelty of this study. The photocatalysts were characterized with FESEM-EDX/TEM, AAS, UV-Vis DRS and XRD equipment. The Pt dispersion or chemisorption active surface area of the as-prepared samples was analyzed using TPDRO equipment. Based on the relevant characterization, the role of Pt depositing methods on TNP was investigated.

2   Material and Methods

2.1   Materials

TiO_2-P25 (TNP, Evonic Degussa Co), chloroplatinic acid (H_2PtCl_6 $6H_2O$, Sigma Aldrich), sodium borohydride ($NaBH_4$, Sigma Aldrich 99%), methanol (Merck, 99% and >99.9%), ethanol (Merck, 96% and >99.5%), and glycerol (Brataco, 98.8%) were bought and used without purification. All solutions used were made using high-purity distilled water.

2.2   Platinized TiO_2 (Pt-TNP)

2.2.1   Chemical Reduction Method

To prepare Pt-TNP-CR, a suspension of 2 g TNP in 400 ml of dilute solution with H_2PtCl_6 as precursor (loading Pt = 1 wt%) was added with $NaBH_4$ in excess and stirred for 1 h. After chemical reduction, the solution was centrifuged for 20 min and the filtrate was washed twice with ethanol and distilled water. The slurry was then evaporated by drying on a temperature-adjustable electric hot plate at 90 °C for about 3 h, heated at 130 °C for 1 h, and finally calcination was performed at 500 °C for 1 h in a furnace. The photocatalyst sample is denoted as Pt-TNP-CR.

2.2.2   Photodeposition

A suspension of 2 g TNP in 360 ml of dilute solution with H_2PtCl_6 as precursor (loading Pt = 1 w%) was added to 40 ml of a water-methanol mixture (10 v/v% methanol). Photodeposition of Pt on TNP was performed for 6 h in a photo reactor that made of Pyrex glass. This reactor was placed inside a reflection box equipped with magnetic stirrer and six UV-A lamps (11 watts). After photodeposition, centrifugation of the solution was executed for 20 min and followed by washing of the filtrate with distilled water. Evaporation of the slurry was followed by calcination, similar to the chemical reduction method. The photocatalyst sample is denoted as Pt-TNP-PD.

2.3   Characterization of Pt-TNP

The surface morphology of the Pt-TNP was examined using a Transmission Electron Microscope (TEM, FEI BM-Eagle Microscope Tecnai 200 kV D2360 SuperTwin). To determine the elemental mapping in the Pt-TNP samples, an energy dispersive X-ray (EDX) analyzer was available in a FESEM (FEI-Inspect F50). The average size of the Pt nanoparticles was calculated by measuring the diameter of each Pt nanoparticle (using the Image J software) and then averaging was done according to the number of existing nanoparticles. Using the Origin software, we determined the Pt size distribution on the TNP. The Atomic Absorption Spectroscopy (AAS Analyst 400 type, Perkin Elmer) was used to measure the real Pt deposited on the prepared Pt-TNP.

TPDRO equipment (Chemisorp 2750, USA Micrometric) was used to measure the chemisorbed surface area of the Pt-TNP by pulse chemisorption based on UOB Method 945-96. First, helium was introduced to the TPDRO quartz reactor containing the Pt-TNP sample, which was heated to 240 °C to remove any adsorbed gases and moisture. The temperature was then increased to 580 °C to remove other species, so that only pure Pt would be loaded on the surface of the TNP. Subsequently, the temperature was allowed to reach room temperature. Introducing a known amount of pure hydrogen (UHP 99.999%) into the TPRDO quartz reactor, which contained a certain amount of the Pt-TNP sample was performed to measure pulse chemisorption. The un-adsorbed residual hydrogen by Pt coming out after chemisorption was measured. Using this method, the amount of chemisorbed hydrogen mass of the sample and Pt loading can be used to calculate the chemisorption surface area. The ratio of H_2 chemisorbed by the photocatalyst with the amount of Pt in the photocatalyst (H_2/Pt) indicates the Pt dispersion in the photocatalyst. If this ratio is equal to 1, 100% of the Pt was dispersed completely.

The crystalline phases of the Pt-TNP were determined using Shimadzu X Ray Diffraction/XRD 7000 with Cu $K\alpha$ ($\lambda = 0.154184$ nm) as the X-ray source, a scan rate of 2° min^{-1} over a 2θ range of 10-80°, operated at 40 kV and 30 mA. The crystallite sizes of the Pt-TNP samples were estimated from full-width at half-maximum (FWHM) by the Scherrer equation. The effect of the Pt deposited on the TNP on the energy bandgap of the Pt-TNP samples, UV-Vis DRS analysis was performed using a Shimadzu spectrophotometer 2450. The reflectance and absorbance of the samples in the wavelength range of 200 to 600 nm were obtained under room temperature.

## 2.4   Photocatalytic H_2 Generation

The photocatalytic H_2 generation experiments were evaluated in a 500 ml Pyrex glass photoreactor that contained 200 ml of glycerol-water mixture with 10 v%

glycerol and was equipped with a mercury lamp (Philips HPL-N 250 W/542 E40 HG ISL, 83% visible and 17% UV light) as photon source and thermocouple. The mercury lamp was placed one cm away from the photoreactor as a photon source to stimulate the reaction. The reactor was placed inside a reflector box and the reactions were performed for 4 h under irradiation. Before the reaction, the Pt-TNP in the reactor flask was magnetically stirred for about 30 min. Subsequently, the photoreactor was flushed with argon/Ag to remove air to avoid disturbance during H_2 generation. Any H_2 generated produces a peak in a Shimadzu Gas Chromatograph (GC 2014 equipped with GC solution software) and the amount of H_2 was estimated from the peak area every 30 min via online sampling. For H_2 and CO_2 analysis, a molecular sieve (MS Hydrogen 5A, 80-100 mesh) column and CO_2 Porapack N packed column (L = 6 m, Di = 2.2 mm) were available in the GC that was interfaced to a personal computer. To obtain the peak/signal of H_2 and CO_2 generated, a Thermal Conductivity Detector (TCD) was employed. The data presented were processed repeatedly. The area of H_2 and CO_2 peaks below 50 counts can be detected with this GC system. High-purity argon (99.99%) was used as carrier gas at 50 cm^3/min.

3   Result and Discussion

3.1   Preparation of Pt Deposited on TNP

The reaction of Pt loading on TiO_2 (TNP) via chemical reduction with chloroplatinic acid as Pt precursor can be described as follows [4,24]:

$$NaBH_4(s) + H_2PtCl_6(s) + H_2O(l) \rightarrow Pt(s) + H_3BO_3(aq) + 5\ HCl(l) +$$

$$NaCl(aq) + 2H_2(g) \tag{1}$$
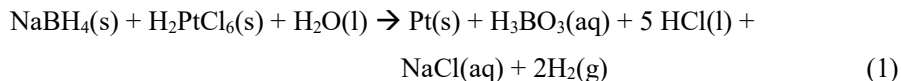
$NaBH_4$ was added into an H_2PtCl_6 solution that had been pre-mixed with TiO_2, leading pH to increase from 5 to 9, as well as color alteration from white to black, indicating that ionic Pt was reduced to metallic Pt. The mixing of Pt with TiO_2 resulted in Pt deposition on the photocatalyst. The photo deposition method, on the other hand, involved the excitation of electrons from TiO_2 VB to CB, and hole scavenging by methanol. Electrons concomitantly reduce ionic Pt according to [4,21]:

$$TiO_2 + (hv) \rightarrow TiO_2\ (e^- + h^+) \tag{2}$$

$$PtCl_6{}^{-2}\ (s) + 4e^- \rightarrow Pt(s) + 6Cl- \tag{3}$$

In-situ reduction of ionic Pt on the TiO_2 surface allows the deposition of Pt on the TiO_2 surface, forming a Pt-TiO_2 composite.

3.2 FESEM/TEM and AAS Analysis

The EDX spectra and elemental mapping of Pt-TNP with 1 wt% Pt loading are presented in Figure 1. These results indicate the presence of Pt on the TNP. According to this data, the Pt was deposited on the TNP, both in case of chemical reduction and photodeposition.
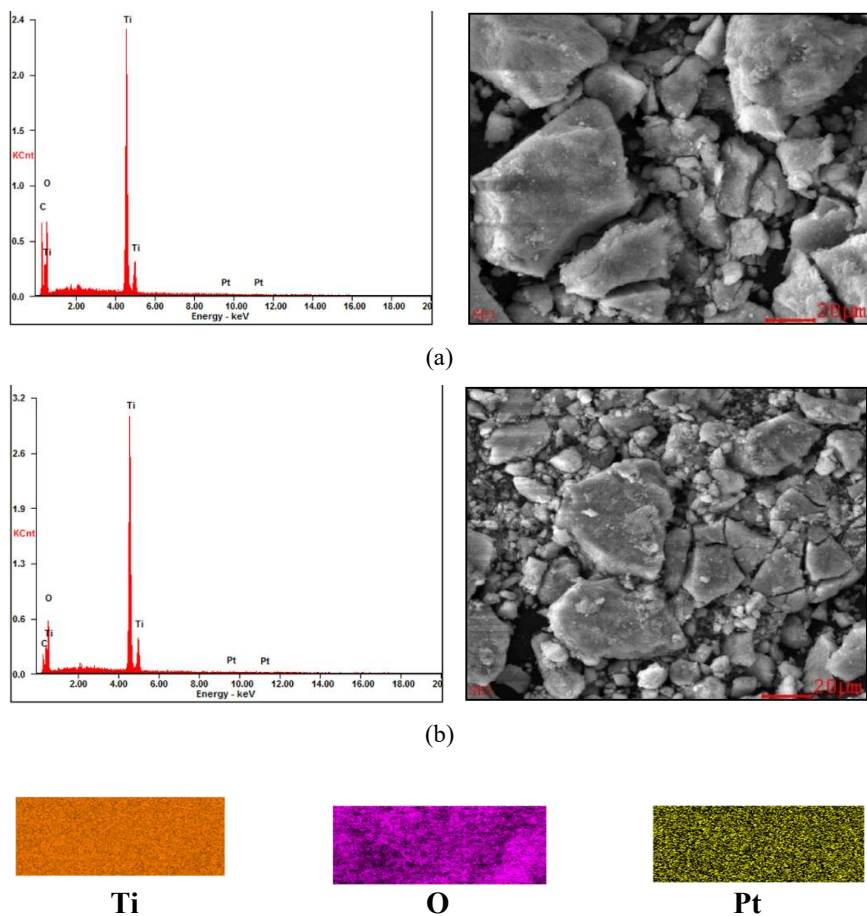

(a)

(b)

Ti   **O**   **Pt**

Figure 1 EDX spectra, SEM image and elemental mapping of synthesized catalyst: (a) Pt-TiO$_2$-CR and (b) Pt-TiO$_2$-PD.
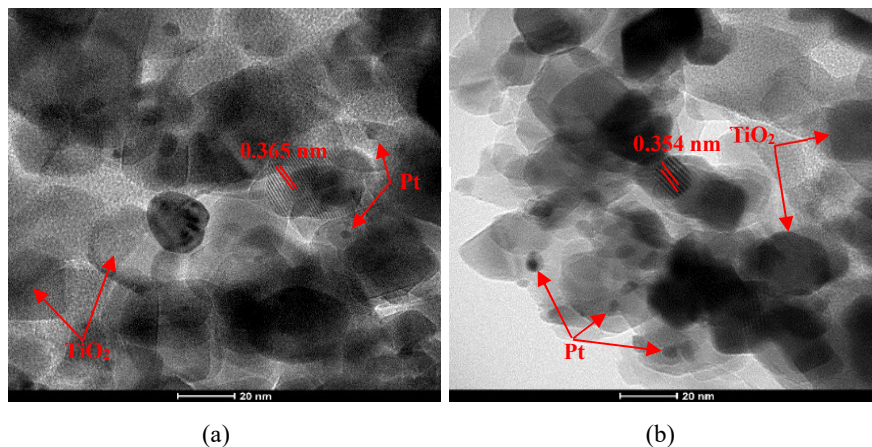
Figure 2 TEM images of: (a) Pt-TiO₂-PD, (b) Pt-TiO₂-CR with small dot nanoparticles showing decorated Pt on the surface of TiO₂ nanoparticles.
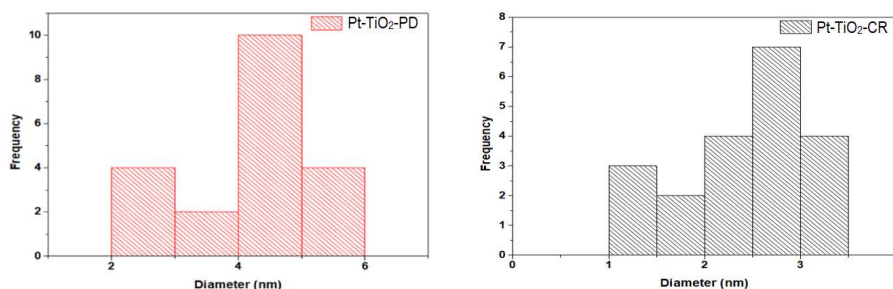

Figure 3 Pt deposit size distribution for Pt-TiO₂-PD and Pt-TiO₂-CR. The number of counts used to determine average Pt deposit size was 20 particles.

3.3   Pt Dispersion Analysis

The degree of dispersion (%) of the Pt on the TNP surface is the ratio between the amount of H_2 adsorbed (chemisorption) by the Pt and the total amount of Pt in the photocatalyst. Table 2 presents the degree of dispersion (%) and the chemisorption surface area of the Pt-TNP. This characterization used the basic calculation of 1 wt% of Pt loading on the TNP.

From Table 2, it can be inferred that the chemical reduction method offered a higher degree of Pt dispersion (82.7%), i.e., 70% more than the photodeposition method (47.8%). As a result, this method presents a higher chemisorbed surface area. The higher the degree of dispersion, the better the photoactivity of the Pt-TNP since it has a larger surface area for reaction sites [6,24,28,29]. The lower Pt dispersion on Pt-TNP-PD could be caused by the lower amount of Pt deposited

on the TNP as shown in the AAS result. If 3.45 ppm of Pt deposited on Pt-TNP-PD gave 47.8% Pt dispersion, 9.48 ppm of Pt deposited on Pt-TNP-CR should give more than 82.7% Pt dispersion. This means that there is little agglomeration on Pt-TNP-CR. Since the Pt-TNP-CR photocatalyst has a smaller Pt particle diameter and this method can deposit a larger amount of Pt on TiO_2, chemical reduction is usually favored over other methods (e.g. evaporation or thermal decomposition). It has been reported that chemical reduction of Pt with precursor H_2PtCl_6 and $NaBH_4$ as reducing agents exhibited 95% dispersion for 1.25% wt of Pt-decorated TiO_2 nanotubes [24]. The chemisorption results (Table 2) were in accordance with the FESEM/TEM/AAS data and give evidence of Pt deposited on TNP. Highly dispersed Pt is better than agglomerated Pt in enhancing the photocatalytic performance on $g-C_3N_4$ [30].

Table 2 Degree of dispersion and Chemisorption surface area of Pt on TNP.

Parameter	Pt-TNP-CR	Pt-TNP-PD	Unit
Degree of dispersion (%)	82.7	47.8	%
Chemisorbed surface area	2.04	1.18	m^2/ g sample

3.4 XRD Analysis

XRD patterns of the photocatalyst samples are depicted in Figure 4. The observed peaks at 2θ of 25.3°, 37.8, 48.0°, 54.3°, 55.05° respectively which conform to anatase phase, correspond to the Miller indices of (101), (004), (200), (105), (221) according to JCPDS No. 21-1272.
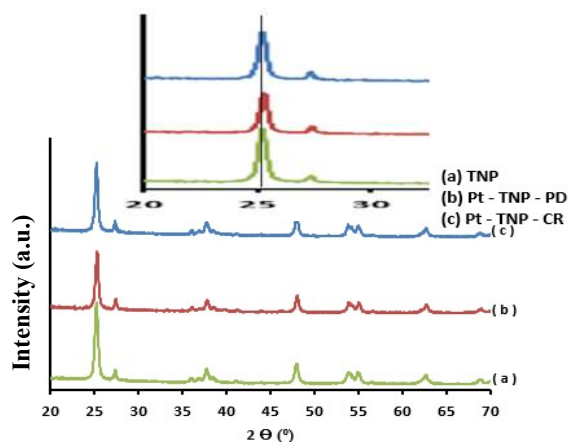

Figure 4 XRD patterns of TNP, Pt-TiO_2-PD, and Pt-TiO_2-CR.

The weak signals at 2θ of 27.4° and 36° conform to rutile phase (JCPDS No. 21-1276) [14]. The amount of Pt loading on TNP (1 wt%) was not enough to induce

diffraction peaks, since Pt peaks would not be found at a low Pt concentration and a high Pt dispersion on TNP [10,21]. A Pt peak appears when Pt loading is 3 wt% at 2θ of 39.8, and 46.4° [23]. The crystallite size of the composites was calculated to be 24, 23, and 29 nm for bare TNP, Pt-TNP-PD and Pt-TNP-CR, respectively, based on applying the Scherrer formula on the broadening of the XRD peak at 25.3°.

The crystalline size is increased with the deposition of Pt on TNP and Pt deposited on TNP could influence the degree of crystallinity and the crystallite size. There was a small shift in the peak position on the Pt-TNP-PD and the Pt-TNP-CR (Figure 4 inset), meaning that Pt deposition alters the lattice parameters of TNP [30]. Meanwhile, the diffraction patterns of the photocatalyst samples were similar.

3.5   Bandgap Analysis

The bandgaps of various photocatalysts estimated by interpretation shown in Figures 5(a) and 5(b) present the UV-Vis absorption spectra of the photocatalyst samples. These results indicate that deposition of Pt on the TNP improved the response to visible light due to the lowered bandgap from 3.25 eV (TNP) to 2.96 eV (Pt-TNP-CR) and 2.98 eV (Pt-TNP-PD). The decrease in bandgap is most likely caused by the deposition of Pt on TNP, as reported by several authors [6,10,16,25]. This phenomenon indicates that the loading of Pt affects the lattice of TNP, which is in line with the XRD results. A similar result, the bandgap of the original anatase TNTA (3.2 eV) was reduced to 2.93 eV after Pt was deposited on the TNTA as previously studied [4]. With a reduced bandgap of Pt-TNP, absorption of photon energy becomes lower for electron excitation, which is thermodynamically advantageous for hydrogen production and leads to high photocatalytic performance under visible light.

The bandgap energy of Pt-TNP-PD is bigger than that of Pt-TNP-CR because of the larger-size metal Pt particles on Pt-TNP-PD (4.4 Nm) compared to the Pt particles on Pt-TNP-CR (2.8 Nm) [25]. The lowering bandgap of Pt-TNP indicates that deposition of Pt on TNP can cause a redshift of photon absorption [6,10,25]. In addition, the ascension of visible-light absorption caused by the incident photon frequency resonates with the collective excitations of electrons of noble-metal nanoparticles on the conduction band. This phenomenon is called localized surface plasmon resonance (LSPR) [31].

A Comparative Study of Pt Depositing Methods (Chemical Reduction Vs Photo-Assisted Deposition) Onto Tio2 Nanoparticle for Hydrogen Photo-Production
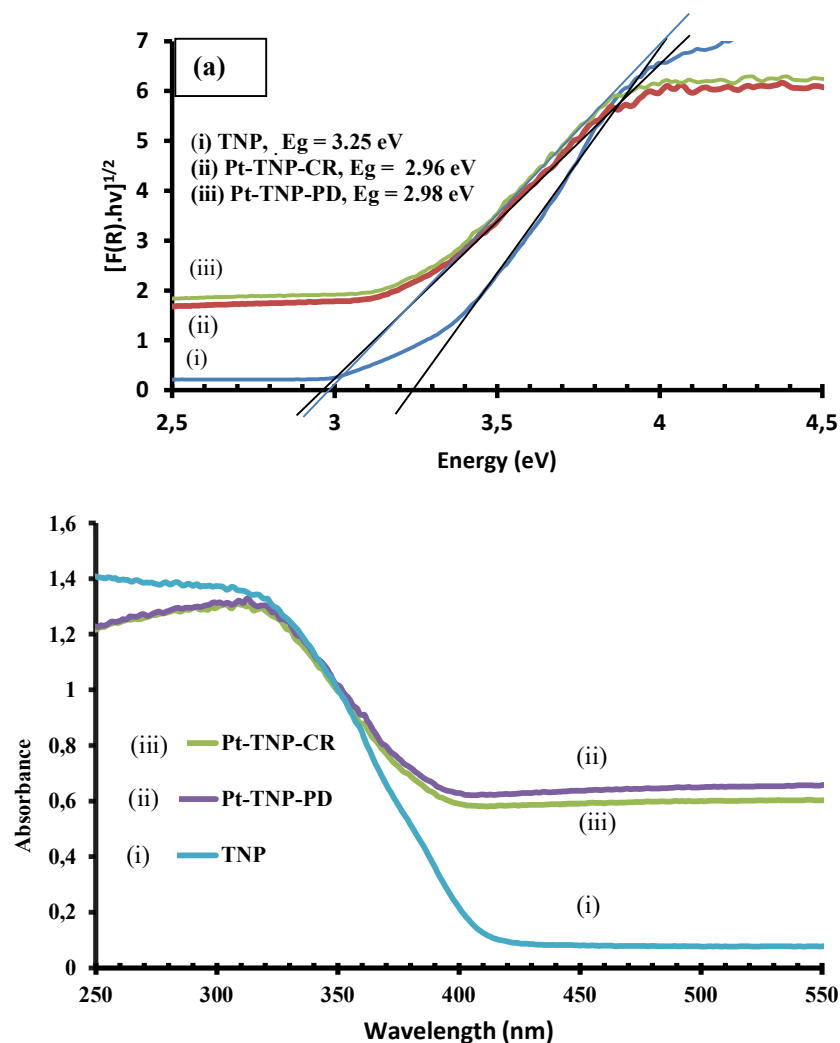

Figure 5 (a) Tauc plot of transformed Kubelka-Munk function vs energy (hv) and (b) UV-Vis absorption spectra for TNP, Pt-TiO$_2$-PD, and Pt-TiO$_2$-CR.

3.6 Photocatalytic Test for H$_2$ Generation

Figure 6 presents the accumulative H$_2$ production (μmol) from the glycerol solution at variation of irradiation time (240 min) for different Pt-TNP samples. From this figure, the rate of hydrogen generation was 97.5, 4104 and 2485

μmol/(h.g catalyst) for the TNP, the Pt-TNP-CR, and the Pt-TNP-PD, respectively. The temperature of the reactor was observed using a thermocouple along the process; it was constant at about 80 °C after 75 min of irradiation. To maintain this condition, an exhaust fan was set up. The 10% glycerol concentration in this study is sufficient to obtain a substantial improvement to photocatalytic H_2 production and represents its concentration in biodiesel waste [4,16].
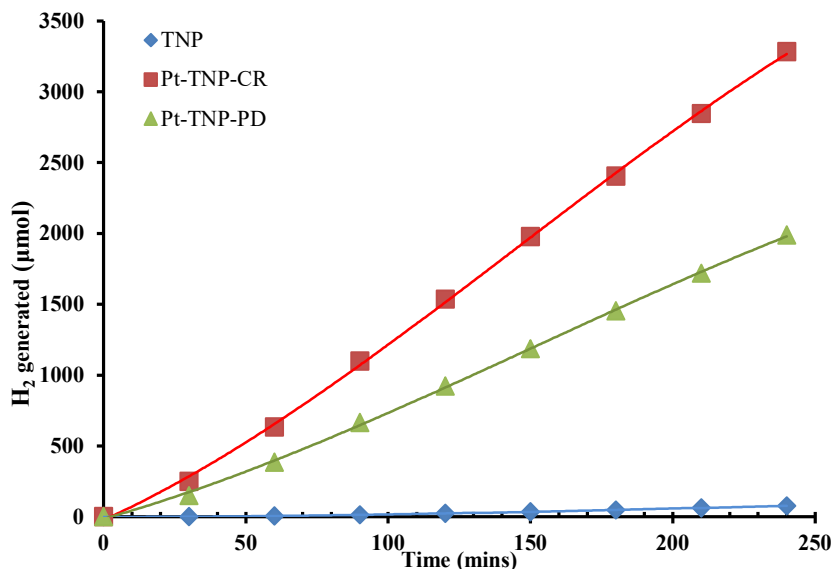

Figure 6 Accumulative H_2 production on the TNP, the Pt-TNP-CR and the Pt-TNP-PD as a function of irradiation time. Suspension volume = 200 ml; catalyst loading = 1 g/L.

The Pt-TNP-CR produced 3283 μmol of H_2, i.e., 1.65 times higher compared to the Pt-TNP-PAD (1988 μmol). These results are significantly higher than those obtained by unmodified TNP (78 μmol). The small H_2 production by pure TiO_2 compared to platinized TiO_2 has also been reported by Xing *et al.* [5,11,21,32]. The enhancement in H_2 production over deposition of Pt on TNP is attributed to the fact that Pt acts as an electron trapper that inhibits electron-hole recombination, thus increasing the photocatalytic activity [6,10]. It is well-documented that electron-hole recombination occurs in the order of ns, while charge conduction occurs in the order of μs or even ms. Therefore, without an electron anchor, photogenerated electron-hole pairs typically undergo unrestricted recombination [24]. The superiority of Pt-TNP-CR over Pt-TNP-PD

1268

A Comparative Study of Pt Depositing Methods (Chemical Reduction Vs Photo-Assisted Deposition) Onto Tio2 Nanoparticle for Hydrogen Photo-Production

in photocatalytically producing H_2 can be ascribed to its higher Pt depositing amount and smaller Pt size, which may lead to better interaction between Pt and CB electrons, as well as with H^+ as a reduction target on the CB. Electron anchoring by Pt requires an abundance of holes available for oxidation in VB, hence improving the reaction rate of glycerol oxidation. As a result, recombination could be suppressed, since more electrons react with H^+, producing H_2, and more holes oxidize glycerol, producing CO_2 and H_2. However, the Pt nanoparticle size in the range of 1-4 nm is not a major determining factor in the photocatalytic production of H_2, as reported by previous researchers [32].

The mechanism of electron trapping and H_2 production on the Pt-TNP is shown in Figure 7. In the context of Pt as an electron trapper, thermodynamic requirements entail that the work function of Pt must be higher than that of TNP [15,26], and the Fermi level of the TNP should be higher than that of the Pt. When Pt particles are coupled with TNP, electron transfer takes place from the CB of the TNP to the Pt until their Fermi levels are aligned or reach the same level [6,33]. As a result, a space charge region is formed on the side of the TNP, which causes an upward bending of the energy band. When the Pt-TNP absorbs photons, electrons are moved from the TNP valence band (VB) to the conduction band (CB) and are subsequently transferred to the Pt, allowing a further upward bending of the energy band over the TNP. Thus, because of the Schottky barrier, the electrons cannot backflow. As a result, electron-hole pair recombination is reduced since the Pt-TNP composite facilitates their separation, which results in boosted photocatalytic activity [34]. Furthermore, the smaller the metal particle size, the greater the shift in Fermi level to the CB, which results in greater photocatalytic reduction efficiency [24,33]. Dispersed Pt on the TNP could also improve the reaction rate of water splitting by reducing the overpotential of proton reduction [15]. Electron transfer from Pt-TNP to H^+ adsorbed species can only occur when the Fermi level of the composite is more negative than the H^+/H_2 reduction potential [24]. In this case, the Pt acts as a co-catalyst for hydrogen production as well as for glycerol photo-oxidation.

The existence of CO_2 was detected by the GC probe, but it was not measured. It gave evidence that photocatalytic reforming of glycerol occurs since it is oxidized by the OH radicals/·OH, hole/h^+, and/or O_2 generated by the water splitting reaction to obtain several intermediate compounds, and finally followed by H_2 and CO_2 generation as the end product [4, 9,15,16]. Thus, the availability of glycerol in the reactant could enhance the photoactivity of TNP, since it is involved in the hole-participated oxidation reaction, which results in reducing electron-hole recombination, avoiding backward reaction regenerating water molecules [4, 9,15,16].
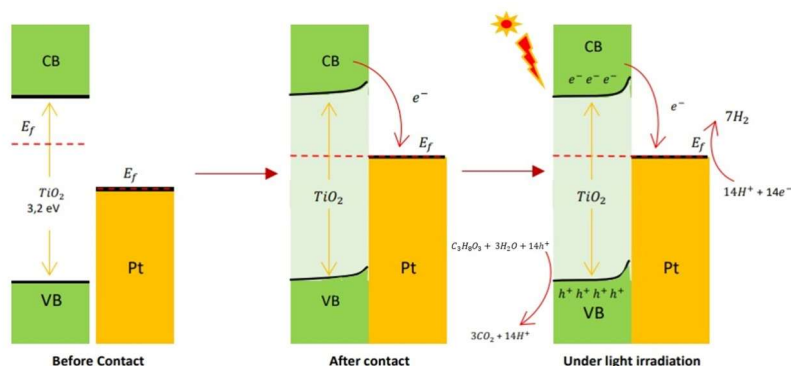
1269

Figure 7 The mechanism of electron trapping and H_2 production on the Pt-TNP before and after coupling under light irradiation, and the redox reaction in the photo-reformation of glycerol.

4   Conclusion

Deposition of Pt on TiO_2-P25/TNP via chemical reduction and photodeposition methods was successfully achieved. The characterization results confirmed that the chemical reduction method offers more efficient Pt deposition and better nano-sized features. Ultimately, Pt-TNP obtained by chemical reduction offers more prominent photocatalytic H_2 production than its counterparts (unmodified TNP and Pt-TNP obtained via photodeposition). Furthermore, decorating Pt on TNP (Pt-TNP) did not affect overall morphology and the structure of the TNP, the data indicated that the band gap was lowered.

Loading 1 wt% of Pt on TNP is necessary since it can inhibit recombination and enhance photocatalytic activity and therefore can increase hydrogen generation from a glycerol-water mixture under visible and UV light as compared to unmodified TNP. Thus, we conclude that the preparation method by which photocatalysts are synthesized plays a major role in the deposition efficiency and the dispersion of Pt particles, which eventually determine H_2 generation activity.

Acknowledgments

A Comparative Study of Pt Depositing Methods (Chemical
Reduction Vs Photo-Assisted Deposition) Onto Tio2 Nanoparticle
for Hydrogen Photo-Production

References

[1] Dincer, J. & Acar, C., *Review and Evaluation of Hydrogen Production Methods for Better Sustainability*, International Journal of Hydrogen Energy, **40**, pp. 11094-11111, 2015.

[2] Fajrina, N. & Tahir, M., *A Critical Review in Strategies to Improve Photocatalytic Water Splitting towards Hydrogen Production*, International Journal of Hydrogen Energy, **44,** pp. 540-577, 2019.

[3] Takata, T., Pan, C. & Domen, K., *Recent Progress in Oxynitride Photocatalysts for Visible-Light-Driven Water Spitting,* Science and Technology of Advanced Materials, **16**, pp. 1-18, 2015.

[4] Slamet, Ratnawati, Gunlazuardi, J. & Dewi, E.L., *Enhanced Photocatalytic Activity of Pt Deposited on Titania Nanotube Arrays for the Hydrogen Production with Glycerol as a Sacrificial Agent,* International Journal of Hydrogen Energy, **42**, pp. 24014-24025, 2017.

[5] Vaiano, V., Lara, M.A., Iervolino, G., Matarangolo, M., Navio, J.A. & Hidalgo M.C., *Photocatalytic H_2 Production from Glycerol Aqueous Solutions Over Fluorinated Pt-Tio_2 with High {001} Facet Exposure*, Journal of Photochemical and Photobiology A: Chemistry, **365**, pp. 52-59, 2018.

[6] Scandura, G., Rodríguez, J. & Palmisano, G., *Hydrogen and Propane Production from Butyric Acid Photoreforming Over Pt-TiO_2*. Fronties in Chemistry**, 7**(563), pp. 1-14, 2019.

[7] Ge, M., Li, Q., Cao, C., Huang, J., Li, S., Zhang, S., Chen, Z., Zhang, K., Al-Dheyap, S.S. & Lai, Y., *One-dimensional TiO_2 Nanotube Photocatalysts for Solar Water Splitting*, Advanced Science, **4**(1), 1600152, 2017.

[8] Chouhan, N., Ameta, R., Meena, R.K., Mandawat, N. & Ghildiyal, R., *Visible Light Harvesting Pt/Cds/Co-Doped ZnO Nanorods Molecular Device for Hydrogen Generation*, International Journal of Hydrogen. Energy, **41**, pp. 2298-2306, 2016.

[9] Yao, Y., Gao, X., Li, Z. & Meng, X., *Photocatalytic Reforming for Hydrogen Evolution: A Review,* Catalysts, **10**(335), pp.1-17, 2020.

[10] Guayaquil-Sosa, J.F., Calzada, A, Serrano, B., Escobedo, S. & de Lasa, H., *Hydrogen Production via Water Dissociation Using Pt–TiO_2 Photocatalysts: An Oxidation–Reduction Network*, Catalysts, **7**(11), 324, 2017.

[11] Li, F., Gu, Q., Niu, Y., Wang, R., Tong, Y., Zhu, S., Zhang, H., Zhang, Z. & Wang, X., *Hydrogen Evolution from Aqueous-Phase Photocatalytic Reforming of Ethylene Glycol Over Pt/Tio_2* Catalysts: *Role of Pt and Product Distribution,* Applied Surface Science**, 391**, pp. 251-258, 2017.

[12] Sola, A.C., Homs, N. & de la Piscina, P.R., *Photocatalytic H₂ Production from Ethanol(Aq) Solutions: The Effect of Intermediate products*. International Journal of Hydrogen Energy, **41**, pp. 19629-19636, 2016.

[13] Pajares, A., Wan,g Y., Kronenberg, M.J., de la Piscina, P,R. & Homs, N., *Photocatalytic H₂ Production from Ethanol Aqueous Solution Using Tio₂ With Tungsten Carbide Nanoparticles as Co-Catalyst*, International Journal of Hydrogen Energy, **45**, pp. 20558-20567, 2020.

[14] Liu, Y., Wang, Z.& Huang, W., *Influences of Tio₂ Phase Structures on the Structures and Photocatalytic Hydrogen Production of CuOx/TiO₂ photocatalysts*, Applied Surface Science, **389**, pp. 760-767, 2016.

[15] Daskalaki, V.M. & Kondarides, D.I., *Efficient Production of Hydrogen by Photo-Induced Reforming of Glycerol at Ambient Conditions*, Catalysis Today, **144**, pp. 75-80, 2009.

[16] Christoforidis, K.C. & Fornasiero, P., *Photocatalytic Hydrogen Production: A Rift into the Future Energy Supply,* Chem Cat Chem, **9**, pp. 1523 – 1544, 2017.

[17] Zhu, Y., Chen, Z., Gao, T., Huang, Q., Niu, F., Qin, L., Tang, P., Huang, Y., Sha, Z & Wang, Y., *Construction of Hybrid Z-Scheme Pt/CdS-TNTAs with Enhanced Visible-Light Photocatalytic Performance*, Applied Catalysis B: Environment, **163**, pp. 16-22, 2015.

[18] Ortiz, A.L., Zaragoza, M.M., Gutierrez, J.S., da Silva Paula, M.M. & Collins-Martı́nez, V., *Silver Oxidation State Effect on the Photocatalytic Properties of Ag Doped TiO₂ for Hydrogen Production under Visible Light*, International Journal of Hydrogen Energy, **40**, pp.17308-17315, 2015.

[19] Wang, Z., Yin, Y., Williams, T., Wang, H., Sun, C. & Zhang, X., *Metal Link: A Strategy to Combine Graphene and Titanium Dioxide for Enhanced Hydrogen Production*, International Journal of Hydrogen Energy, **41**, pp.22034-22042, 2016.

[20] Du, J., Wang, H., Yang, M., Zhang, F., Wu, H. & Cheng, X., *Highly Efficient Hydrogen Evolution Catalysis Based on MoS₂/CdS/TiO₂ Porous Composites*, International Journal of Hydrogen Energy, **43**, pp. 9307-9315, 2018.

[21] Lakshmanareddy, N., Rao, V.N., Cheralathan, K.K., Subramaniam, E.P. & Shankar, M.P., *Pt/TiO₂ Nanotube Photocatalyst – Effect of Synthesis Methods on Valance State of Pt and Its Influence on Hydrogen Production and Dye Degradation*. Journal of Colloid Interface Science, **538**, pp. 83-98, 2019.

[22] Jitan, S.A., Palmisano, G. & Corrado Garlisi, C., *Synthesis and Surface Modification of TiO₂-Based Photocatalysts for the Conversion of CO₂,* Catalysts, **10**(2), 227, 2020.

[23] Gao, H., Zhang, P., Hu, J., Pan, J., Fan, J. & Shao, G., *One-Dimensional Z-Scheme Tio₂/WO₃/Pt Hetero Structures for Enhanced Hydrogen Generation*, Applied Surface Science, **391**, pp. 211-217, 2017.

[24] Anthony, R.P., Mathews, T., Ramesh, C., Murugesan, N., Dasgupta, D., Dhara, S., Dash, S. & Tyagi, A.K., *Efficient Photocatalytic Hydrogen Generation by Pt Modified Tio$_2$ Nanotubes Fabricated by Rapid Breakdown Anodization*, International Journal of Hydrogen Energy, **37**, pp. 8268-8276, 2012.

[25] Khan, M.A., Akhtar, M.S., Wo, S.I. & Yong, O.B., *Enhanced Photoresponse under Visible Light in Pt Ionized TiO$_2$ Nanotube for the Photocatalytic Splitting of Water*, Catalysis Communications, **10**, pp. 1-5, 2008.

[26] Zhang, L., Pan, N. & Lin, S., *Influence of Pt Deposition on Water Splitting Hydrogen Generation by Highly-Ordered TiO$_2$ Nanotube Arrays,* International Journal of Hydrogen Energy, **39**, pp. 13474-13480, 2014.

[27] Lee, J. & Choi, W., *Photocatalytic Reactivity of Surface Platinized TiO$_2$, Substrate Specificity and the Effect of Pt Oxidation State*, Journal of Physical Chemistry B, **109,** pp. 7399-7406, 2005.

[28] Notodarmojo, S., Sugiyana, D., Handajani, M., Kardena, M. & Larasati, M., *Synthesis of TiO$_2$ Nanofiber-Nanoparticle Composite Catalyst and Its Photocatalytic Decolorization Performance of Reactive Black 5 Dye from Aqueous Solution*, Journal of Engineering and Technology Science, **49**, pp. 340-356, 2017.

[29] Mas'udah, K. W., Taufiq, A. & Sunaryono, *The Potential of Corncobs in Producing Reduced Graphene Oxide as a Semiconductor Material,* Journal of Engineering Technology Science, **54**, pp. 220-201, 2022

[30] Liu, M., Xia, P., Zhang, L., Cheng, B. & Yu, J., *Enhanced Photocatalytic H$_2$-Production Activity of G-C$_3$N$_4$ Nanosheets via Optimal Photodeposition of Pt as Cocatalyst.* ACS Sustainable Chemical Engineering, **6**, pp.10472-10480, 2018.

[31] Reddy, N.L., Kumar S., Krishnan, V., Sathish, M. & Shankar M.V.V., *Multifunctional Cu/Ag Quantum Dots on TiO$_2$ Nanotubes as Highly Efficient Photocatalysts for Enhanced Solar Hydrogen Evolution,* Journal of Catalysis, **350**, pp.226–239, 2017.

[32] Xing, J., Li, Y.H., Jiang, H.B., Wang, Y. & Yang, H.G., *The Size and Valence State Effect of Pt on Photocatalytic H$_2$ Evolution over Platinized TiO$_2$ Photocatalyst,* International Journal of Hydrogen Energy, **39**, pp.1237-1242, 2014.

[33] Vaidyanathan, S., Eduardo, E.W. & Prashant, V.K., *Catalysis with TiO$_2$/Gold Nanocomposites Effect of Metal Particle Size on the Fermi Level Equilibration*, Journal of the American Chemical Society, **126**, pp. 4943-4950, 2004.

[34] Xia Y., Cheng, B., Fan, J., Yu, J. & Liu G., *Near-infrared Absorbing 2D/3D Znin$_2$s$_4$/N-Doped Graphene Photocatalyst for Highly Efficient CO$_2$ Capture and Photocatalytic Reduction*, Science China Materials, 2020: **63**(4), pp 552–565, 2020.